Condition Monitoring of Squirrel-Cage Induction Motors Fed by PWM -based Drives Using a Parameter Estimation Approach

Behrooz Mirafzal, Fariba Fateh, ChiaChou Yeh, Richard Povinelli, and Nabeel A. O. Demerdash

Department of Electrical and Computer Engineering
Marquette University
Milwaukee, WI 53233, USA

***Abstract* - A rotor condition monitoring technique is presented in this paper based on a parameter estimation approach. In this technique, the stator currents, voltages and motor speed are used as the input signals, where the outputs will be the rotor's inductance, resistance and consequently rotor time constant. This approach is verified by simulation of two different induction motor cases. These simulations are buttressed by experimental data obtained for a 2-hp induction motor in the case of healthy as well as one, three and five rotor bar breakages. In these tests, the induction motor was energized from a PWM-based drive, in order to demonstrate the capability of using this method for rotor condition monitoring purposes.**

***Keywords:* Parameter estimation, condition monitoring, rotor time constant, induction motors, rotor broken bar detection.**

I. INTRODUCTION

In the literature, there are many papers regarding rotor condition monitoring, and rotor fault detection [1-6]. Some of these works have mainly used the frequency spectrum of the stator current for rotor condition monitoring. The rotor magnetic field orientation pendulous oscillation, due to broken bars, was recently presented as an index for rotor fault diagnostic purposes. There are other techniques which are based on the artificial intelligence and data mining methods as well as some investigations based on parameter estimation or parameter identification techniques.

A reliable parameter estimation technique for induction motors is critical for the development of high-performance drive systems, and it can also be utilized for condition monitoring applications as well. However, in the context of existing literature the main thrust of parameter estimation techniques in motor-drive control applications is its use to achieve fast and controlled torque response of an induction motor utilizing the principle of vector (field oriented) control. The widely used squirrel-cage rotor aids in the robustness and economy of the drive, but rotor quantities are not accessible. However, the full advantage of vector control is available only if the instantaneous position of the rotor flux vector relative to a stationary reference frame can be indirectly obtained. Hence, knowledge of motor parameters is needed.

This paper is based upon work supported by the National Science Foundation under Grant No. ECS-0322974.

An accurate parameter estimation technique can also be used for motor condition monitoring purposes [6]. Here in this paper, a simple and reliable technique, based on parameter estimation methods, is introduced for rotor broken bar fault detection. The main idea is that the apparent rotor resistance and leakage inductance of a squirrel-cage induction motor will increase when a rotor bar breaks. Meanwhile, the stator resistance, inductance and the magnetizing inductance will not be directly impacted by such rotor bar breakages. This will be justified here from experimental laboratory observations. It is a well established fact that a broken bar fault generates modulation envelops superposed on the amplitudes of stator currents over a slip cycle. This type of envelops can not be observed under no-load condition because the squirrel-cage bars virtually conduct no current under such a condition. Accordingly, the rotor circuit's effects are hardly reflected on the stator side. This means that the stator parameters are not affected by a bar breakage. This is due to the fact that in a no-load situation only the electrical circuits of the stator windings carry the currents and the rotor circuit behaves like an open circuit secondary winding.

This paper addresses two issues, first it presents a new approach for rotor parameter estimation of induction motors, and second it presents the utilization of this parameter estimation approach for purposes of rotor condition monitoring of induction motors.

The present rotor parameter estimation approach constitutes a combination of signal processing and least squares techniques. In this approach, the motor terminal currents, voltages and motor speed are sampled over a specific period of time. The measured voltages and currents are transformed from an ABC frame of reference to a *stationary* dq0 reference frame. Then, the obtained voltages and currents are further broken down to their frequency components. Furthermore, those waveforms are mathematically expressed in a form of summation of sinusoidal waveforms with their associated frequencies. Consequently, the rotor currents, which are not physically accessible, can be calculated. Based on the measured stator quantities and obtained rotor currents, all represented in the stationary dq0 reference frame, a least squares method was implemented to calculated the rotor's inductance and resistance estimations.

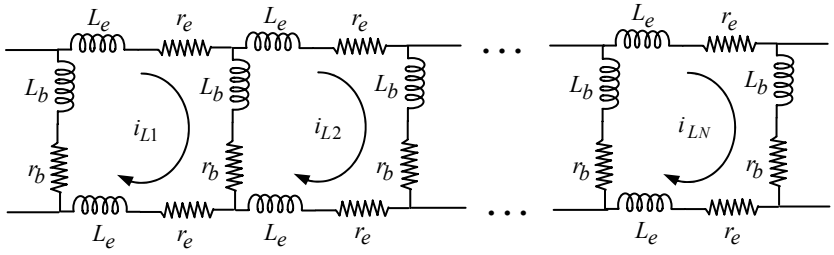

Fig.1 The developed squirrel-cage rotor circuit representation.

II. The Induction Motor Model

The matrix equation of the induction motor in a dq0 reference frame can be expressed as follows [7]:

$$\begin{bmatrix} v_{qs} \\ v_{ds} \\ 0 \\ 0 \end{bmatrix} = \begin{bmatrix} r_s + L_s D & \omega L_s & L_m D & \omega L_m \\ -\omega L_s & r_s + L_s D & -\omega L_m & L_m D \\ L_m D & (\omega - \omega_r) L_m & r_r + L_r D & (\omega - \omega_r) L_r \\ -(\omega - \omega_r) L_m & L_m D & -(\omega - \omega_r) L_r & r_r + L_r D \end{bmatrix} \begin{bmatrix} i_{qs} \\ i_{ds} \\ i_{qr} \\ i_{dr} \end{bmatrix} \quad (1)$$

where, r_s is the stator resistance, r_r is the rotor resistance, L_s is the stator inductance, L_r is the rotor inductance, L_m is the magnetizing inductance, ω_r is the rotor speed, ω is the speed of the reference frame, and D is the time differential operator.

This matrix equation can be represented in a dq0 reference frame fixed to the stator, by substituting the reference frame speed, $\omega = 0$ in (1), which leads to the following:

$$\begin{bmatrix} v_{qs} \\ v_{ds} \\ 0 \\ 0 \end{bmatrix} = \begin{bmatrix} r_s + L_s D & 0 & L_m D & 0 \\ 0 & r_s + L_s D & 0 & L_m D \\ L_m D & -\omega_r L_m & r_r + L_r D & -\omega_r L_r \\ \omega_r L_m & L_m D & \omega_r L_r & r_r + L_r D \end{bmatrix} \begin{bmatrix} i_{qs} \\ i_{ds} \\ i_{qr} \\ i_{dr} \end{bmatrix} \quad (2)$$

The first two rows of (2), which express the stator differential equations, can be rewritten as follows:

$$Di_{qr} = \frac{1}{L_m}\left(v_{qs} - r_s i_{qs} - L_s Di_{qs}\right) \quad (3)$$

$$Di_{dr} = \frac{1}{L_m}\left(v_{ds} - r_s i_{ds} - L_s Di_{ds}\right) \quad (4)$$

Here, v_{qs}, v_{ds}, i_{qs}, i_{ds}, i_{qr}, and i_{dr} are represented in the stationary frame of reference with the rotor currents referred to the stator side. Using the Fast Fourier Transformation (FFT), one can obtain all frequency components of any stator or rotor voltages and currents. From the obtained frequency components, the waveforms can be reconstructed in a time domain as the summation of the sinusoidal waveforms. For instance, the i_{qs} can be expressed as follows:

$$i_{qs} = \sum_{h=1}^{m} I_{qs(h)} \cos\left(\omega_{iqs(h)} t + \psi_{iqs(h)}\right) \quad (5)$$

therefore, Di_{qs} can be simply obtained by the following expression:

$$Di_{qs} = \sum_{h=1}^{m} -I_{qs(h)} \omega_{iqs(h)} \sin\left(\omega_{iqs(h)} t + \psi_{iqs(h)}\right) \quad (6)$$

Again, the main idea is that the apparent rotor resistance and inductance of a squirrel-cage induction motor will increase when a rotor bar breakage occurs. This becomes obvious upon examination of the developed circuit representation of the rotor cage, see Fig.1, in which one or more bar breakages will mean that one or more of the bar resistances, r_b, will assume an infinite value. Consequently, and increase in the overall equivalent resistance of the rotor cage will ensue. Meanwhile, such a bar breakages will have virtually no effect on stator resistance, stator leakage inductance and the magnetizing inductance which are depend on stator condition and load. Hence, these parameters are considered as the known parameters which might be calculated off-line through the no-load and locked rotor tests, or other techniques.

Substituting the terms, v_{qs}, v_{ds}, i_{qs}, i_{ds}, Di_{qs}, and Di_{ds} into (3) and (4) gives a series of digital values for Di_{qr} and Di_{dr}. Furthermore, those can be represented as the summation of sine-waves. For instance, Di_{qr} can be written as follows:

$$Di_{qr} = \sum_{h=1}^{m} \tilde{I}_{qr(h)} \cos\left(\omega_{iqr(h)} t + \psi_{iqr(h)}\right) \quad (7)$$

therefore, the rotor currents, i_{qr}, can be calculated as follows:

$$i_{qr} = \sum_{h=1}^{m} \frac{\tilde{I}_{qr(h)}}{\omega_{iqr(h)}} \sin\left(\omega_{iqr(h)} t + \psi_{iqr(h)}\right) \tag{8}$$

A similar procedure can be achieved for calculating i_{dr} from Di_{dr}. Now, the next step is to calculate r_r and L_r based on the known quantities, which are v_{qs}, v_{ds}, i_{qs}, i_{ds}, Di_{qs}, Di_{ds}, Di_{qr}, Di_{dr}, i_{qr}, and i_{dr} in a specific period of time in the form of series of digital values. From (2), the rotor differential equations can be rewritten as follows:

$$i_{qr} r_r + (Di_{qr} - \omega_r i_{dr}) L_r = \omega_r L_m i_{ds} - L_m Di_{qs} \tag{9}$$

$$i_{dr} r_r + (Di_{dr} + \omega_r i_{qr}) L_r = -\omega_r L_m i_{qs} - L_m Di_{ds} \tag{10}$$

where, the unknown parameters are the rotor resistance, r_r, and the rotor inductance, L_r. In order to estimate these parameters, either (9) or (10) can be used for implementing a Least Squares (LS) method. Here, equation (9) is considered for the remainder of the discussion on estimating the unknown parameters. Let vectors, θ, and x, and scalar, y be defined as follows:

$$\theta = \begin{bmatrix} \theta_1 & \theta_2 \end{bmatrix}^T = \begin{bmatrix} r_r & L_r \end{bmatrix}^T,$$

$$x = \begin{bmatrix} x_1 & x_2 \end{bmatrix}^T = \begin{bmatrix} i_{qr} & Di_{qr} - \omega_r i_{dr} \end{bmatrix}^T,$$

$$y = L_m (\omega_r i_{ds} - Di_{qs}).$$

Hence, (9) can be expressed based on the vectors of the unknown parameter, θ, x, and y as follows:

$$x^T \theta = y \tag{11}$$

in this case, $y \in \mathbb{R}^1$, $\theta \in \mathbb{R}^2$, and $x \in \mathbb{R}^2$.

Since, θ contains two elements, if we sampled the system at two different instants, t_k, t_{k+1}, one can write the following:

$$\begin{bmatrix} x_1(t_k) & x_2(t_k) \\ x_1(t_{k+1}) & x_2(t_{k+1}) \end{bmatrix} \begin{bmatrix} \theta_1 \\ \theta_2 \end{bmatrix} = \begin{bmatrix} y(t_k) \\ y(t_{k+1}) \end{bmatrix} \tag{12}$$

or we can write $X\theta = Y$ and if X is non-singular, then it follows that $\hat{\theta} = X^{-1} Y$. Of course the estimated vector parameters will not be exactly equal to the real values, this means $\hat{\theta} \neq \theta$, because the x's and the y's contain measurement noise. If we made N measurements, $N > 2$, we could minimize the squared error between the actual output, $y(t_k)$, and the predicted output, $\hat{y}(t_k) = \hat{\theta}^T x(t_k)$, by minimizing:

$$J(\hat{\theta}) = \frac{1}{N} \sum_{k=1}^{N} \alpha \left[y(t_k) - \hat{\theta}^T x(t_k) \right]^2 \tag{13}$$

where, α is known as the weighting factor and typically $(1/\alpha)$ is set to a value just less than one. After further mathematical manipulation the following formulations are obtained (see Appendix for more details):

$$\hat{\theta}(t_k) = \hat{\theta}(t_{k-1}) + P(t_k) x(t_k) \alpha \left[y(t_k) - (\hat{\theta}(t_{k-1}))^T x(t_k) \right] \tag{14}$$

where,

$$P(t_k) = P(t_{k-1}) - \frac{P(t_{k-1}) x(t_k) (x(t_k))^T P(t_{k-1})}{(x(t_k))^T P(t_{k-1}) x(t_k) + (1/\alpha)} \tag{15}$$

It has to be pointed out that the denominator in (15) is a scalar, although x is a vector, and P is a matrix. Typically, $P(t_0) = CI_{2\times 2}$, where, C is a large constant number, and the initial estimated values are set to be $\hat{\theta}(t_0) = [0 \quad 0]^T$.

The approach procedure can be summarized in the following functional block diagram shown in Fig.2.

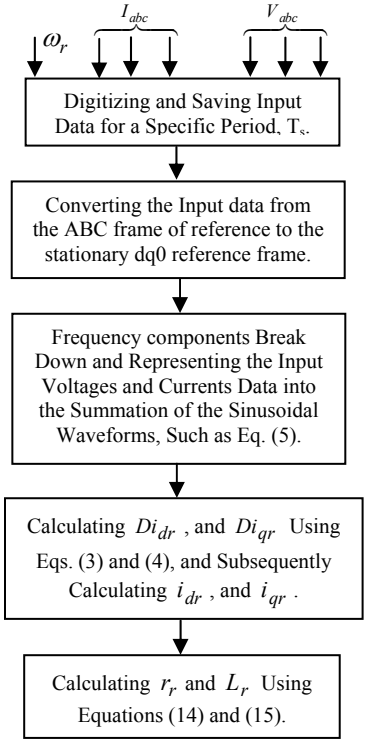

Fig.2. The approach procedure

III. Simulation Results

Before implementing this new approach for the condition monitoring of the rotor cage of an induction motor, this approach was examined for two different sizes of induction motors, where their respective rated values and their parameters are given in Table 1.

TABLE I
INDUCTION MOTORS PARAMETERS

Motor Rating			r_s	L_s	L_m	L_r'	r_r'	J
hp	volts	rpm	(ohms)	(H)	(H)	(H)	(ohms)	(kg.m^2)
7.5	220	1710	0.35	0.0540	0.0525	0.0532	0.25	0.026
50	460	1705	0.09	0.0390	0.0375	0.0384	0.15	0.047

The simulation results were obtained during the stating transient period of each induction motor, when the induction motor was energized by a three-phase sine-wave voltage source. Here, in Fig.3 and Fig.4, the rotor estimated resistance and the rotor estimated inductance of the 7.5-hp power induction motor are shown as an example. The actual parameters, the final estimated values, e.g. see Fig.3, and the errors of these estimations for both the 7.5-hp and 50-hp are given in Table 2 and Table 3.

The simulation results show that the percentage errors between the actual and estimated rotor inductances are 0.38% and 0.26% for the 7.5-hp and 50-hp induction motors, respectively. However, the percentage errors between the actual and estimated rotor resistances are 3.48% and 9 % for the 7.5-hp and 50-hp induction motors, respectively. This means that both the estimated resistances and inductances are very close to the actual corresponding values.

In order to investigate which one of the rotor parameters are more suitable for rotor condition monitoring purposes, a white noise was added to the actual speed. This means that a random value between 0 and 1 % of the rated speed was added to the actual speed value. The estimation results, which are given in Table 4 and Table 5, show that the estimated value of rotor inductance is more reliable than the estimated rotor resistance value.

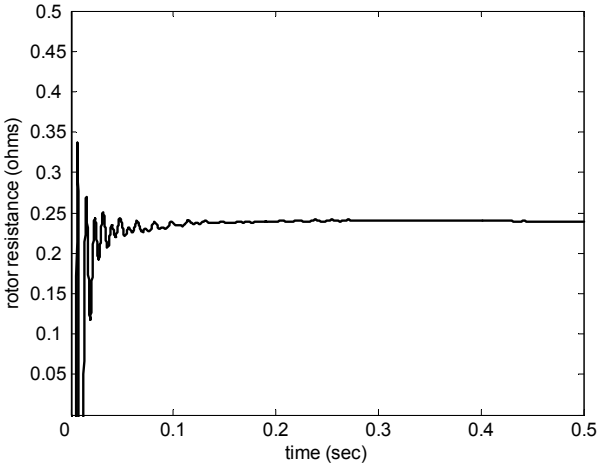

Fig.3. The rotor resistance estimation of the 7.5-hp induction motor during motor staring.

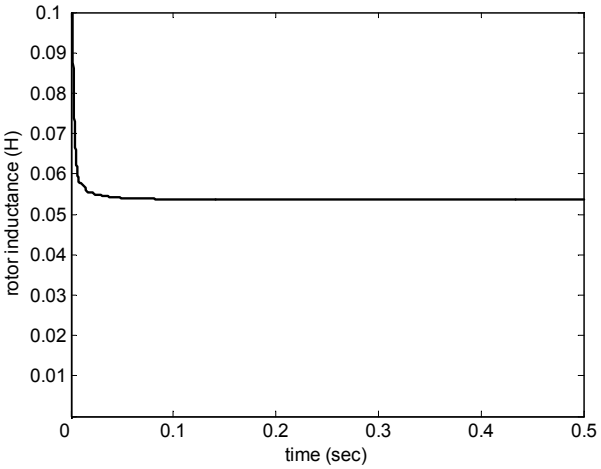

Fig.4. The rotor inductance estimation of the 7.5-hp induction motor during motor starting.

TABLE II
ROTOR ACTUAL AND ESTIMATED RESISTANCE

Induction Motor	Actual Value	Estimated Value	Error
7.5-ph	0.25	0.2413	3.48 %
50-hp	0.15	0.1363	9 %

TABLE III
ROTOR ACTUAL AND ESTIMATED INDUCTANCE

Induction Motor	Actual Value	Estimated Value	Error
7.5-hp	0.0532	0.0534	0.38 %
50-hp	0.0384	0.0385	0.26 %

TABLE IV
ROTOR ACTUAL AND ESTIMATED RESISTANCE
IN PRESENCE OF NOISE IN THE SPEED MEASUREMENTS

Induction Motor	Actual Value	Estimated Value	Error
7.5-ph	0.25	0.2312	7.52 %
50-hp	0.15	0.1355	9.67 %

TABLE V
ROTOR ACTUAL AND ESTIMATED INDUCTANCE
IN PRESENCE OF NOISE IN THE SPEED MEASUREMENTS

Induction Motor	Actual Value	Estimated Value	Error
7.5-hp	0.0532	0.0527	0.94 %
50-hp	0.0384	0.0381	0.78 %

IV. Experimental Results

In addition to the simulation verification of the new approach for rotor parameters estimation, a set of experimental data obtained from testing a 2-hp induction motor with 36 rotor bars, stator resistance 0.65 ohms, and magnetizing inductance, 0.165 (H), was implemented for further verification. . These tests were done under healthy condition as well as one, three and five broken bars conditions in a steady state situation, when the motor was energized by a PWM-based drive with a constant Volts/Frequency control strategy. In these tests, the output line frequency of the drive was set to 50 Hz, when the carrier frequency was 1.2 KHz. Here, the acquired data was recorded during steady state. In this case the instantaneous values for speed measurement were not available, hence an average value for speed was assumed in each case. However, the terminal voltages and currents was sampled through a very accurate data acquisition laboratory setup, LabView SCXI 1140, when sampling rate was set to 50K sample per second. The test phase voltage and current waveforms for the healthy motor are shown in Fig.5 and Fig.6, respectively. Meanwhile, the modulated envelop over a slip cycle in the stator current due to three rotor broken bar fault is demonstrated in Fig.7. Here, the rotor parameter estimation results based on these experimental data are give in Table 6.

TABLE VI
ROTOR ESTIMATED INDUCTANCES OF 2-HP-IM
(EXPERIMENTAL RESULTS)

Case Study	Estimated Values
Healthy Cage	0.1662
One Broken Bar	0.1663
Three Broken Bars	0.1665
Five Broken Bars	0.1668

V. Conclusion

A simple and reliable rotor parameter estimation approach has been presented in this paper. It has been found that this approach can be used for the rotor condition monitoring purposes. The estimated rotor inductance indicates that this parameter increases in value with an increase in the number of broken bars. Moreover, from the simulation and experimental results, it has been found that estimation of the rotor inductance is more reliable than the rotor resistance, especially when a noise exists in the speed measurements

.

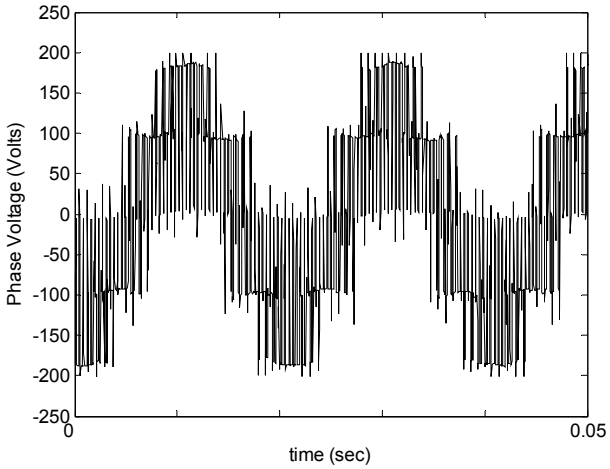

Fig.5. The stator phase voltage waveform of the 2-hp induction motor during steady state, (healthy case).

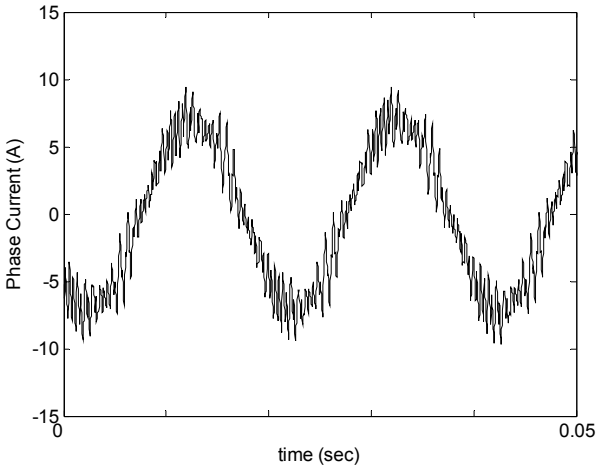

Fig.6. The stator phase current waveform of the 2-hp induction motor during steady state, (healthy case).

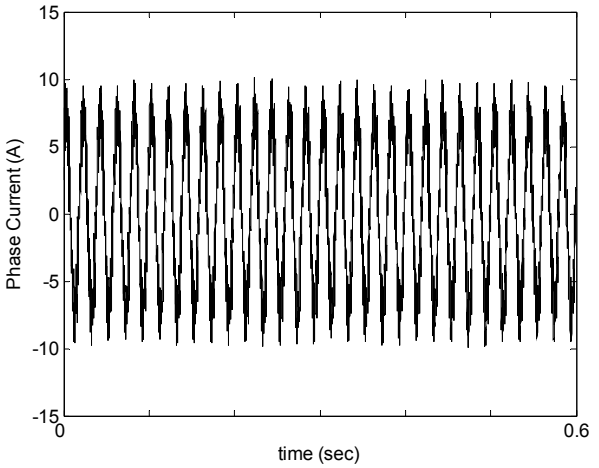

Fig.7. The stator phase current waveform of the 2-hp induction motor during steady state over a slip cycle, (Three broken bars).

APPENDIX

In order to minimize "*the squared error between the actual output,* $y(t_k)$*, and the predicted output,* $\hat{y}(t_k) = \hat{\theta}^T x(t_k)$," which is:

$$J(\hat{\theta}) = \frac{1}{N}\sum_{k=1}^{N} \alpha_k \left[y(t_k) - \hat{\theta}^T x(t_k) \right]^2$$

one can write the following:

$$\frac{\partial J(\hat{\theta})}{\partial \hat{\theta}} = -\frac{2}{N}\sum_{k=1}^{N} \alpha_k \left[y(t_k) - \hat{\theta}^T x(t_k) \right] (x(t_k))^T = 0$$

or,

$$\sum_{k=1}^{N} \alpha_k \hat{\theta}^T x(t_k)(x(t_k))^T = \sum_{k=1}^{N} \alpha_k y(t_k)(x(t_k))^T$$

this yields:

$$\begin{aligned}
\hat{\theta}(N) &= \overbrace{\left[\sum_{k=1}^{N} \alpha_k x(t_k)(x(t_k))^T \right]^{-1}}^{R^{-1}(N)} \left[\sum_{k=1}^{N} \alpha_k y(t_k) x(t_k) \right] \\
&= R^{-1}(N) \left[\sum_{k=1}^{N-1} \alpha_k y(t_k) x(t_k) + \alpha_N y(t_N) x(t_N) \right] \\
&= R^{-1}(N) \left[\left(R(N-1)\ \hat{\theta}(N-1) \right) + \alpha_N y(t_N) x(t_N) \right]
\end{aligned}$$

note that, $R(N-1) = R(N) - \alpha_N x(t_N)(x(t_N))^T$, therefore:

$$\hat{\theta}(N) = \hat{\theta}(N-1) + R^{-1}(N) x(t_N) \alpha_N \left[y(t_N) - (x(t_N))^T \hat{\theta}(N-1) \right]$$

this can be further simplified, let define $P = R^{-1}$, hence

$$P(N) = \left[P^{-1}(N-1) + \alpha_N x(t_N)(x(t_N))^T \right]^{-1},$$

using the following linear algebra formula:

$$\left[A + BCD \right]^{-1} = A^{-1} - A^{-1} B \left[DA^{-1}B + C^{-1} \right]^{-1} DA^{-1},$$

it follows that :

$$P(N) = P(N-1) - \frac{P(N-1)x(t_N)(x(t_N))^T P(N-1)}{(x(t_N))^T P(N-1) x(t_N) + (1/\alpha_N)},$$ and

$$\hat{\theta}(N) = \hat{\theta}(N-1) + P(N) x(t_N) \alpha_N \left[y(t_N) - (\hat{\theta}(N-1))^T x(N) \right].$$

ACKNOWLEDGMENT

The Authors would like to thank Dr. Ronald Brown for his helpful discussions on using the least squares method.

REFERENCES

[1] S. Williamson and A.C. Smith, "Steady state analysis of 3-phase cage motors with rotor-bar and end-ring faults" *Proc. Inst. Elec. Eng*., vol. 129, no. 3, pp.93-100, 1982.

[2] G. B. Kliman, R.A. Koegl, J. Stein, R. D. Endicott, and M.W. Madden, "Noninvasive detection of broken bars in operating induction motors," *IEEE Transactions on Energy Conversion*, vol. 3, No.4, pp. 873-874, Dec. 1989.

[3] M. Haji, H. A. Toliyat, "Pattern recognition - A technique for induction machines rotor broken bar detection," *IEEE Transactions Energy Conversion*, vol. 16, No. 4, December 2001.

[4] J. F. Bangura, R. J. Povinelli, N. A. O. Demerdash, R. H. Brown. "Diagnostics of eccentricities and bar/end-ring connector breakages in polyphase induction motors through a combination of time-series data mining and time-stepping coupled FE-state space techniques," *IEEE Trans. on Ind. Appl*., vol. 39, pp. 1005-1013, July/August 2003.

[5] B. Mirafzal, N. A. O. Demerdash, " Induction machine broken-bar fault using the rotor space-vector magnetic field orientation," *IEEE Transactions On Industry Applications*, vol., No., pp., March/April 2004.

[6] M. S. N. Said, M. E. H. Benbouzid, A. Benchaib, "Detection of broken bars in induction motors using an extended Kalman Filter for rotor resistance sensorless estimation," *IEEE Transactions on Energy Conversion*, vol. 15, No.1, pp. 66-70, March, 2000.

[7] P. C. Krause, O. Wasynczuk, and S. D. Sudhoff, Analysis of Electric Machinery and Drive Systems. IEEE Press, 2002.